

Geomechanical Properties from Drilling Data to Optimize Stimulation Design

Mazeda Tahmeen, Rocsol Technologies Inc.; Alexandra E. Cedola and Geir Hareland, Oklahoma State University; John P. Hayes, Rocsol Technologies Inc.

Copyright 2019, AADE

This paper was prepared for presentation at the 2019 AADE National Technical Conference and Exhibition held at the Hilton Denver City Center, Denver, Colorado, April 9-10, 2019. This conference is sponsored by the American Association of Drilling Engineers. The information presented in this paper does not reflect any position, claim or endorsement made or implied by the American Association of Drilling Engineers, their officers or members. Questions concerning the content of this paper should be directed to the individual(s) listed as author(s) of this work.

Abstract

Recent studies suggested that selective stimulations could significantly increase production rates at a reduced cost. In this article, a convenient technology is presented that uses surface drilling data to calculate the geomechanical properties for optimizing stimulation design. The technology uses a 3D wellbore friction model to estimate the effective downhole weight on bit (DWOB) from the surface measurements of directional drilling. The estimated DWOB is used as an input to the inverted rate of penetration model to calculate the geomechanical properties such as, the unconfined compressive strength (UCS), Young's modulus (E), porosity, permeability and Poisson's ratio. The stimulation index (STIX) can be obtained from the calculated geomechanical properties as well, to investigate the rock fracability in unconventional hydrocarbon reservoirs.

The study wells A and B were investigated to calculate the geomechanical properties from horizontal drilling in the Montney shale formation in NEBC (North East British Columbia, Canada). The routinely collected depth- and time-based drilling data were used to estimate the DWOB and there from the geomechanical properties at each drilled depth. The calculated geomechanical properties were compared to the available test analysis on cores. In addition, the rock mechanical and reservoir property log including the stimulation index, STIX of Well C in the lower Eagle Ford formation was calculated as well.

In unconventional reservoir this technology can be used to engineer stimulation design by selecting sweet spots from the recognized behavior of the geomechanical properties. This novel technology could help geologists and reservoir engineers to optimize selective stimulation design leading to increased production rates and a greater net present value (NPV).

Introduction

Thousands of wells are drilled and completed annually in unconventional hydrocarbon reservoirs, especially in North America. Generally, little information is known about the mechanical and geological properties of the reservoir rocks needed to identify the fracturing intervals to optimize the completion and production from the individual wells producing from these reservoirs. This is primarily due to the lack of core analysis and logging data on these wells and in most cases these wells are completed with a geometric evenly spaced fracture. A more detailed reservoir characterization allows for an optimal

stimulation design through selective perforations versus the geometric spacing method. An investigation on the effectiveness of the selective stimulation revealed that the initial gas flow back rates from the wells stimulated by the engineered completions were 33% to 40% higher than the geometrically completed well and therefore suggest better reservoir contact and higher productions (Ajayi et al., 2013). In addition, the concept of rock brittleness was investigated from the geomechanical data to identify the effective zones in unconventional reservoirs (Rickman et al., 2008) for optimal stimulation design and it was also revealed that brittle rocks are easier to fracture (Zehnder, 2012).

Detailed logging and core information needed to selectively perforate and potentially optimize the stimulation treatment, is typically collected in one of twenty wells, primarily because of the higher expense and time required for conventional logging techniques. Furthermore, the geomechanical and geological information is inaccurately extrapolated from the offset vertical wells, thus leading to less effective stimulation design for the lateral and highly deviated horizontal wells drilled in unconventional reservoirs. Logging techniques that are accurate and cost-effective for obtaining a continuous geomechanical property log as well as a better understanding of effective downhole conditions have become widely investigated in the oil and gas industry within recent years.

While drilling wells in the unconventional reservoir, drilling data are collected as a standard practice both in time and as a function of measured depth. In recent years, researchers and engineers have been focusing on the use of routinely acquired drilling data to investigate effective logging techniques. Downhole drilling conditions, including the downhole weight on the drill bit and rock strengths can be predicted utilizing available drilling data. With extended reach (ER) horizontal drilling, the actual DWOB differs from the surface weight on bit (WOB) due to the friction caused by drillstring movement, rotation within the wellbore and wellbore geometry. A three-dimensional (3D) torque and drag (T&D) model was developed to estimate the coefficient of friction and effective DWOB from the surface measurements of WOB (SWOB), hook load, surface applied RPM along with the wellbore survey measurement, standpipe pressure and drill string information (Aadnoy et al., 2010). The formation rock strength in the term of confined compressive strength (CCS) and therefrom UCS, can be

obtained from the inverted drill bit rate of penetration (ROP) models (Hareland et al., 2010). Quantico solution technologies output the synthetic logs using surface measurements and neural network algorithms. The Completion Optimization While Drilling (COWD) technology also utilizes drilling data to calculate the corrected mechanical specific energy (CMSE) which is used to obtain fracture index and geomechanical logs (Jacques et al., 2017).

Unlike the use of neural networks and the concept of CMSE, a convenient and data-driven D-Series logging technology is presented that uses the 3D T&D model to estimate the effective DWOB profile from horizontal well drilling data, which is an important input parameter in the inverted ROP model. The inverted ROP model is integrated with drill bit cutting effects, bit wear as a function of rock abrasiveness, and the effect of bit hydraulics to calculate more accurate strength logs, including, CCS, UCS, Young's Modulus (Tahmeen et al., 2017). This article introduces a complete geomechanical property log including the rock strengths, porosity, permeability, Poisson's ratio and there from the concept of rock brittleness and STIX using routinely available drilling data and formation specific constants.

D-Series Technology

The D-Series technology consists of two application modules, D-WOB and D-ROCK as illustrated in Figure 1. The routinely acquired time- and depth-based drilling data along with drill string information and survey data are the inputs to the D-WOB module. The output of the D-WOB module (DWOB), the drill bit data and mud report (available in the daily drilling report) are the inputs to the D-ROCK module which is used to calculate rock mechanical and reservoir properties at each drilled depth. The mathematical models and other correlations used in the D-Series technology, are discussed in the following sections.

Wellbore Friction Model for D-WOB Module

The 3D T&D model (Aadnoy et al., 2010 and Fazaelizadeh et al., 2010) was developed by considering an element of the drillstring (DS) in the wellbore filled with drilling fluid and wellbore geometry. The forces considered on the drillstring element are buoyed weight, axial tension, friction force and normal force perpendicular to the contact surface of the wellbore as shown in Figure 2. Figure 2(a) and Figure 2(b) represent the element with straight inclined section and curved section respectively, along the DS from the surface to the total depth (TD).

While lowering the DS, the force balance on a straight inclined drillstring element is (Aadnoy et al., 2010 and Fazaelizadeh et. al., 2010):

$$F_{top} = \beta w \Delta L (\cos \alpha - \mu \sin \alpha) + F_{bot} \quad (1)$$

For a curved section when the DS is in tension, the force balance for lowering the DS is:

$$F_{top} = \beta w \Delta L \left[\left(\frac{\sin \alpha_t - \sin \alpha_b}{\alpha_t - \alpha_b} \right) + \mu \left(\frac{\cos \alpha_t - \cos \alpha_b}{\alpha_t - \alpha_b} \right) \right] + F_{bot} (e^{-\mu|\theta|}) \quad (2)$$

where,

$$\theta = \cos^{-1} \left[\frac{\sin \alpha_t \sin \alpha_b \cos(\varphi_t - \varphi_b) + \cos \alpha_t \cos \alpha_b}{1} \right] \quad (3)$$

For a curved section in compression, the force balance on a DS element for lowering, is (Johancsik et al., 1984):

$$F_{top} = \beta w \Delta L \left[\cos \left(\frac{\alpha_t + \alpha_b}{2} \right) \right] - \mu F_n + F_{bot} \quad (4)$$

where,

$$F_n = \left[\begin{array}{l} \left\{ F_{bot} (\varphi_t - \varphi_b) \sin \left(\frac{\alpha_t + \alpha_b}{2} \right) \right\}^2 \\ + \left\{ F_{bot} (\alpha_t - \alpha_b) + \beta w \Delta L \sin \left(\frac{\alpha_t + \alpha_b}{2} \right) \right\}^2 \end{array} \right]^{1/2} \quad (5)$$

The D-WOB module uses Eq. (1) to Eq. (5) for calculating the coefficient of friction when the drill bit is off-bottom lowering, and the effective DWOB when the drill bit is on-bottom for the drilling process.

Inverted ROP Model and Other Correlations for D-ROCK Module

The ROP models for PDC (Polycrystalline diamond compact) and Rollercone drill bits consider the effects of bit wear, drilling parameters, such as pump flow rate and RPM, and drill bit cutting structure (Hareland and Nygaard, 2007, Kerkar et al., 2014 and Rashidi et al., 2015). By rearranging the ROP models, the rock strength (CCS) can be defined as follows:

$$CCS = \left(\frac{ROP}{K \times DWOB^{b_1} \times RPM^{c_1} \times h_x \times W_f \times B_x} \right)^{\frac{1}{a_1}} \quad (6)$$

UCS and Young's modulus (E) can be defined as,

$$UCS = CCS / (1 + a_s \times P_c^{b_s}) \quad (7)$$

$$E = CCS \times a_E \times (1 + P_c)^{b_E} \quad (8)$$

The porosity (ϕ) and permeability (K_P) correlations for the shale formation was obtained from various shale cores and cuttings analysis (Cedola et al., 2017a and Cedola et al., 2017b) as given below:

$$\phi = k_{por1} \times UCS^{-k_{por2}} \quad (9)$$

$$K_P = k_{prm3} \times \phi^{k_{prm4}} \quad (10)$$

Here a_s , b_s , a_E , b_E , k_{por1} , k_{por2} , k_{prm3} and k_{prm4} are reservoir specific formation constants calculated using laboratory triaxial test data on reservoir core samples.

Poisson's ratio is an important elastic property of reservoir rock needed for stimulation design and is a measure of the compressibility of the material perpendicular to the applied stress. The rock (Mohr) failure envelope method was used to obtain the angle of internal friction (β) and therefrom the coefficients of earth at rest (K_0) and Poisson's ratio (ν) (Hareland and Hoberock, 1993):

$$\beta = \sin^{-1} \left[1 / \left(1 + \left\{ \frac{4\Delta}{u_{CS} \times a_S \times [P_{e1}^{b_S} - P_{e2}^{b_S}]} \right\} \right) \right] \quad (11)$$

$$K_0 = 1 - \sin \beta; \quad \nu = \frac{K_0}{1 + K_0} \quad (12)$$

The D-ROCK module uses Eq. (6) to Eq. (12) to generate a complete geomechanical property log utilizing drilling data while drilling a horizontal well in an unconventional reservoir. The constants used in Eq. (6) to Eq. (12) are required to calibrate for the specific reservoir formation.

Calculation of DWOB from Drilling Data

The field data from three sample wells in North America were used to verify the model algorithms of D-Series technology by generating the downhole property logs for the wells. Well A and Well B are in the Montney shale formation and Well C is in the Eagle Ford formation. For this study, the available depth-based and time-based drilling data for the three test wells and the corresponding directional survey data were collected from the data service providers. The information of drillstring components, including BHA (bottom hole assembly), regular drill pipes and heavy weight drill pipes used along the horizontal wellbores were obtained from the operator's daily drilling/operation reports. The input data files were formatted as per the requirements of the D-Series modules and D-WOB functional tools were used to perform necessary data quality controls (QCs) to avoid any wrong calculations from bad raw inputs. The coefficient of friction (CF) was calculated along the three horizontal wellbores utilizing the corresponding time-based off-bottom drilling data and therefrom the effective DWOB were obtained using the depth-based on-bottom drilling data and other required inputs. Figure 3 shows the comparison of the calculated DWOB profiles with the corresponding SWOB of well A, well B (in metric units) and well C (in imperial units). The blue plots and red plots in Figure 3 represent the SWOB and the calculated DWOB, respectively. The CF was calibrated before each drilling mode and the calculated DWOBs of the three wells were observed between 64% to 85% of the SWOB. The spikes in the WOB profiles of Well A and Well C represent the higher WOB in the on bottom sliding modes. For the selected drilled depth between 2650m to 3450m in the lateral section of Well A, the CF was estimated between 0.08 to 0.17 and the effective DWOB was observed between 64% to 85% of the corresponding SWOB with an average of around 73.6%. The DWOB profile calculated using the T&D model was verified with the corresponding DWOB measurements using the CoPilot

downhole tool, as shown in Figure 4. Figure 4(a) represents the rotary RPM profile while drilling and therefore the lower values near zero RPM represent the sliding sections within the selected drilled depth. The DWOB measurement using the CoPilot downhole tool is presented by the green plots in Figure 4(b) and Figure 4(c). The sliding sections in Figure 4(b) show higher values of both SWOB (blue plot) and DWOB (red plot). Figure 4(b) shows a good match in the rotary drilling sections, but there is a significant difference between the calculated DWOB (red plot) in sliding sections and the corresponding DWOB measurements (green plot). It reveals that the T&D model calculates DWOB accurately in the rotary drilling sections but not in the sliding sections. Therefore, the calculation of sliding DWOB was adjusted to obtain a better match in the sliding sections as well.

A sliding model was developed as a function of differential pressure (DP) across the mud motor and a sliding constant K_{SLD} (Wu and Hareland, 2015) as defined below:

$$DWOB_{Sliding} = K_{SLD} \times DP \quad (13)$$

The sliding constant K_{SLD} , can be obtained from the relationship between the differential pressures and the corresponding T&D model-based DWOBs calculated at the rotary drilling section just before the specific sliding section. The calculated DWOB using the sliding model in the sliding sections as well as using the T&D model in the rotary drilling sections gives a more accurate match (red plot) with the DWOB data (green plot) as shown in Figure 4(c).

Calculations of Geomechanical Properties

The calculated DWOB (output from the D-WOB module) was applied to the inverted ROP model for the PDC drill bit to generate the rock mechanical and reservoir property log utilizing the D-ROCK module of the D-Series technology. The D-WOB output, drilling data and additional required inputs from the sample horizontal wells in the Montney and Eagle Ford formations in North America were used in this analysis.

The drill bit input files were generated from the available bit reports utilizing the D-ROCK bit editor tool. In addition, the formation constants required to calculate the rock mechanical and reservoir properties were obtained from available laboratory test data on cores or drill cuttings utilizing the formation constants regression analysis tools in D-ROCK. For example, the constants defined in Eq. (7), Eq. (8), Eq. (9) and Eq. (10) for the NEBC Montney formation, were obtained by the method shown in Figure 5. Figure 5(a) and Figure 5(b) represent the regression analysis plots to obtain the formation constants a_S , b_S , a_E and b_E utilizing the D-ROCK functional tools. The laboratory test data on NEBC Montney core samples were collected from external resources. A set of sample formation constants calculated for the Montney shale reservoir is listed in Table 1.

The rock mechanical and reservoir properties for the drilling data of Well A in the NEBC Montney shale formation, was generated utilizing the D-ROCK module as depicted in Figure

6. The estimated DWOB profile of Figure 4(c) considering both rotary drilling and sliding modes, was used to calculate the UCS and therefrom Young's modulus, porosity, permeability and Poisson's ratio through the horizontal wellbore of well A. In Figure 6, the first four plots represent the calculated UCS, Young's modulus, ROP and the calculated DWOB profiles, respectively. The last three plots represent the corresponding permeability, porosity and Poisson's ratio profiles calculated for the specific depth interval drilled through the horizontal wellbore of Well A in the Montney shale formation. The lower window of Figure 6 shows the average calculations summary for the geomechanical properties of Montney shale based on study well A.

For the Montney shale formation, Davey (2012) reported UCS ranging from 117 MPa to 136 MPa and Duenas (2014) reported the Young's modulus being between 35 GPa to 55 GPa. The calculated rock mechanical and reservoir properties used to characterize the unconventional NEBC Montney and Eagle Ford shale reservoirs are summarized in Table 2. In this study, the average UCS and Young's modulus for Well A were found to be 123.24 MPa and 36.7 GPa, respectively, and the results are in good agreement with the reported rock properties as mentioned above. Furthermore, the average calculated porosity and permeability were found to be 2.92% and 199.7 nD respectively, whereas the porosity and the average permeability were reported to be 2% to 5% and 130 nD, respectively, for the Montney shale formation (Duenas, 2014). With this information it can be seen that the model results are in good agreement with the reported values from published data.

The UCS, Young's modulus and permeability were found to range between 53.2 MPa to 129.8 MPa, 16.1 GPa to 41.8 GPa and 273.6 nD to 1247.4 nD respectively, while performing a similar investigation for the horizontal wellbore of Well C. The average porosity was found to be 6.59% and the Poisson's ratio was obtained in the range between 0.221 to 0.356. Sone (2012) reported the Young's modulus for the lower Eagle Ford to range between 25 to 34 GPa. Walls (2011) investigated the rock properties on core samples from two wells in the Eagle Ford utilizing the Digital Rock Physics (DRP) process and reported the average porosity to be 6.9% and the permeability around 300 nD to 1100 nD based on porosity-permeability cross plots.

Investigations of the relationship between UCS-permeability and porosity-permeability cross-plots are widely used to characterize unconventional reservoirs for optimal stimulation design. The flow unit is a function of porosity and permeability leading to pore scale modeling calculations for pore throats (rt) and an approximated porosity-permeability cross-plot with various flow units was introduced for tight and shale hydrocarbon reservoirs based on the investigations of enormous amounts of unconventional hydrocarbon reservoirs worldwide (Aguilera, 2013). The calculated porosities and permeabilities for the NEBC Montney (Well A) and Eagle Ford (Well C) reservoirs provide consistent porosity-permeability cross-plots near the average trend of shale reservoirs for flow units as shown in Figure 7(c). This figure indicates smaller pore throat sizes ranging between 0.009 to 0.1 micrometers (purple

diamond marker) for both study formations.

Rock brittleness is an important factor for characterizing unconventional shale reservoirs for optimal stimulation design. Young's modulus and Poisson's ratio cross-plots are good indicators of rock brittleness, or the ability of rock to fail under load and maintain the fracture (Rickman et. al., 2008 and Bai, 2016). Figure 8 represents the graphical concept of rock brittleness for the Montney (Well A) and lower Eagle Ford (Well C) formations. The rock is more brittle with a higher Young's modulus and a lower Poisson's ratio. Higher brittleness indicates a greater ability of the rock to fracture under load which results in an effective hydraulic fracturing treatment.

Investigations of factors influencing optimal stimulation design for higher production rates suggested that engineered completions are more effective than nonengineered completions in unconventional reservoirs (Ajayi et al., 2013). It is suggested that the effective fracable intervals should be intervals with lower UCS whereas higher UCS and increased effective normal stress are related to the less fracable intervals (Bai, 2016).

Based on the above discussions and in an attempt to develop and integrate a more useful geomechanical property log into the D-ROCK platform for the selective stimulation design and engineered completions, the authors investigated the effective fracable index, STIX. In this analysis, STIX is defined as a function of rock brittleness (ratio of Young's modulus and Poisson's ratio), UCS, porosity and permeability as below:

$$STIX = \frac{E}{\nu} \times UCS^{-a_x} \times \phi^{b_x} \times K_p^{c_x} \quad (14)$$

Here a_x , b_x and c_x are empirical constants and should be calibrated based on the geomechanical analysis for the specific reservoir formation. Different operators might use these coefficients with different goals for the different formations in terms of looking to stimulate stiffer/brittle rock or higher permeability/porosity zones. The unique potential use of these coefficients is that they can be optimized for each individual reservoir in terms of net present value (NPV).

In this analysis, the values of a_x , b_x and c_x are calibrated as 1.5, 1.0 and 1.0, respectively for the lower Eagle Ford formation considering the metric units of the associated reservoir properties. A complete geomechanical property log including the new fracable index, STIX, was investigated utilizing the drilling data along the horizontal wellbore of Well C. The STIX is normalized to define its values between 0 and 1. The value of normalized STIX approaching 1 (one) indicates higher STIX and potentially more fracable rock whereas the value approaching 0 (zero) indicates lesser fracability of the reservoir formation. The graphical representation of the normalized STIX profile along with the corresponding UCS, porosity and permeability profiles from the D-ROCK platform for a sample depth interval (Well C) is shown in Figure 9. The recommended stimulation locations for the selective engineered completion should be the depth intervals with higher STIX and lower UCS in addition to higher porosity and permeability zones

determined from D-ROCK. The intervals with low STIX, high UCS, low porosity and low permeability should be avoided.

Geomechanical Properties for Optimal Stimulation

In recent years hydraulic fracture design considerations for horizontal wells are either a geometric design or an engineered design. Figure 10 represents two hydraulic fracture simulation models for a horizontal well in the Eagle Ford formation (Ajayi et al., 2013). The top simulation model (A) was developed for a geometric design with uniformly distributed fracture stages and perforation clusters, irrespective of the reservoir quality (RQ) and completion quality (CQ) properties such as rock strength, Young's modulus, porosity, permeability, Poisson's ratio and stress components. The bottom engineered design (B) represents the selective location and length of fracture stages and the placement of perforation clusters based on the inputs of rock mechanical and reservoir properties along the horizontal well. The inputs of two aforesaid design analysis were collected utilizing conventional and expensive logging techniques.

Further investigations of a shale formation revealed the optimal stimulation with an engineered completion design leads to economic hydrocarbon production as listed in Table 3 (Ajayi et al., 2013). In Table 3, Well 1, Well 2 and Well 3 were drilled and completed using a geometric or nonengineered stimulation design. Well 4, Well 5 and Well 6 were drilled and completed using an engineered selective stimulation design. The "Completion Summary" and "30-Day Cumulative Production" in Table 3 indicate a more effective completion design in that lower breakdown pressures, higher pumping rates, more effective proppant placement from the wells drilled and completed using an engineered selective stimulation design are achieved based on the geomechanical properties in the shale formation.

The geomechanical properties obtained from drilling data utilizing the novel D-Series technology can be used as inputs to commercially available reservoir and completion models to investigate the engineered stimulation design along the lateral length of a horizontal well thus leading to optimal and economic completion practices in unconventional reservoirs.

Conclusions

A convenient and cost-effective logging technology was presented and applied to three sample wells in North America in order to obtain geomechanical properties from routine drilling data. The wellbore friction model and an inverted ROP model were used to calculate the effective DWOB as well as rock mechanical and reservoir properties. A good agreement was observed between the estimated DWOB for well A and the corresponding DWOB obtained using a downhole measuring tool (CoPilot).

The calculated geomechanical properties were in good agreement with laboratory analysis of rock properties on reservoir specific core samples. Although these investigations reveal encouraging results, some disagreements were also observed which may be due to data uncertainty and complexity of data measurements while drilling the ER horizontal wellbores in unconventional shale reservoirs.

A more detailed reservoir characterization utilizing a complete geomechanical property log can lead to optimal stimulation design through selective perforations and engineered completion in comparison to the current conventional practice of geometric or nonengineered completion. The D-Series geomechanical logs could be used to evaluate unconventional reservoirs and perform wellbore stability analysis by Mechanical Earth Model (MEM) as well as, to map sweet spots and optimize the hydraulic fracturing process for maximizing well productivity.

Research and development will continue to verify the model algorithms as well as the development of the technological capabilities of D-WOB and D-ROCK and integration of the STIX into the D-Series platform. Future work will include integrating the specific optimal stimulation constants in STIX for specific reservoirs which could depend on the individual operator's stimulation goals and NPV. The operators will have the option to include or eliminate this effect as per their requirements.

Nomenclature

$a_1, b_1, c_1 =$ Drill bit constants

$a_E, b_E, a_S, b_S =$ Formation constants obtained from regression analysis

$a_X, b_X, c_X =$ Formation constants for STIX correlation

$B_x =$ Function of drill bit properties

$CQ =$ Completion quality properties; Young's modulus, Poisson's ratio, strength etc.

$D_b =$ Diameter of drill bit

$E =$ Young's modulus

$F_{top}, F_{bot} =$ Force or hook load at top and bottom of the drill string element, respectively

$F_n =$ Net normal force acting on the drillstring element

$GPa =$ Gigapascal

$h_x =$ Hydraulic efficiency function

$K =$ Empirical constant in ROP model

$K_p =$ Permeability

$K_{SLD} =$ Sliding (model) constant

$k_{por1}, k_{por2}, k_{prm3}, k_{prm4} =$ Formation constants for porosity and permeability correlations

$\Delta L =$ Element length of drill string

$Mpa =$ Megapascal

$nD =$ Nanodarcy

$P_c =$ Confining pressure

RQ = Reservoir quality properties; porosity, permeability, fluid saturations etc.

$STIX$ = Stimulation index

w = Unit weight of drillstring element

W = Buoyed weight

W_f = Bit wear function

α_t, α_b = Inclination at top and bottom of the drillstring element, respectively

β = Buoyancy factor

φ_t, φ_b = Azimuth at top and bottom of the drillstring element, respectively

\emptyset = Porosity

μ = Coefficient of friction, CF

ν = Poisson's ratio

θ = Dogleg angle

References (In alphabetical order)

- Aadnoy, B. S., Fazaelizadeh, M. and Hareland, G.: "A 3-Dimensional analytical model for wellbore friction". Journal of Canadian Petroleum Technology, Vol. 49, Issue 10, page 25-36, 2010.
- Aguilera, R.: "Flow units: from conventional to tight-gas to shale-gas to tight-oil to shale-oil reservoirs". SPE 165360, The SPE Western Regional & AAPG Pacific Section Meeting, 2013 Joint Technical Conference, 19-25 April, Monterey, California, USA, 2013.
- Ajayi, B., Aso I. I., Caplan, J., Clark, B. D., Li, X., Liu, H., Luo, Y. and Waters, G.: "Stimulation design for unconventional resources". Oilfield Review Summer, 25, No. 2, 2013.
- Bai, M.: "Why are brittleness and fracability not equivalent in designing hydraulic fracturing in tight shale gas reservoirs". Southwest Petroleum University. Production and hosting by Elsevier B.V. on behalf of KeAi Communications Co. Ltd., 2016.
- Cedola, A. E., Atashnezhad, A. and Hareland, G.: "Evaluating multiple methods to determine porosity from drilling data". SPE Oklahoma City Oil and Gas Symposium, 27-30 March, Oklahoma City, Oklahoma, USA, 2017a.
- Cedola, A. E., Atashnezhad, A. and Hareland, G.: "Real-time porosity from surface drilling data prediction and verification". AADE-17-NTCE-134, 2017 AADE National Technical Conference and Exhibition, 11-12 April, Houston, Texas, USA, 2017b.
- Davey, H.: "Geomechanical characterization of the Montney shale northeast Alberta and northwest British Columbia, Canada", M.S. Thesis, Department of Geology and Geological Engineering, Colorado School of Mines, 2012.
- Duenas, C.: "Understanding rock quality heterogeneity of Montney shale reservoir, Pouce Coupe field, Alberta, Canada". M.S. (Geophysics) Thesis, Faculty and the Board of Trustees, Colorado School of Mines, 2014.
- Fazaelizadeh, M., Hareland, G. and Aadnoy, B. S.: "Application of new 3-D analytical model for directional wellbore friction". Journal of Modern Applied Science, 4: 2, 2-22, 2010.
- Hareland, G. and Nygaard, R.: "Calculating unconfined rock strength from drilling data". ARMA-07-214, 1st Canada-US Rock Mechanics Symposium, 27-31 May, Vancouver, Canada, 2007.
- Hareland, G. and Hoberock, L.: "Use of drilling parameters to predict in-situ stress bounds". SPE 25727, SPE/IADC Drilling Conference, Amsterdam, Netherlands, 1993.
- Jacques, A., Quenes, A., Dirksen, R., Paryani, M., Rehman, S. and Bari, M.: "Completion optimization while drilling – geomechanical steering towards fracable rock using corrected mechanical specific energy". URTeC-2693870, Unconventional Resources Technology Conference (URTeC) 2017, 24-26 July, Austin, Texas, USA, 2017.
- Johancsik, C. A., Friesen, D. B. and Dawson, R.: "Torque and drag in directional wells – prediction and measurement". Journal of Petroleum Technology, SPE 11380, 987-992, 1984.
- Kerkar, P., Hareland, G., Fonseca, E. and Hackbarth, C.: "Estimation of Rock Compressive Strength Using Downhole Weight-On-Bit and Drilling Models". IPTC 17447, International Petroleum Technology Conference, 20-22 January, Doha, Qatar, 2014.
- Rashidi, B., Hareland, G., Wu, Z.: "Performance, Simulation and Field Application Modeling of Rollercone Bits". Journal of Petroleum Science and Engineering, 133-(2015) 507-517, 2015.
- Rickman, R., Mullen, M., Petre, E., Grieser, B. and Kundert, D.: "A practical use of shale petrophysics for stimulation design optimization: All shale plays are not clones of the Barnett shale". SPE 115258, The 2008 SPE Annual Technical Conference and Exhibition, 21-24 September, Denver, Colorado, USA, 2008.
- Sone, H.: "Mechanical properties of shale gas reservoir rocks and its relation to the in-situ stress variation observed in shale gas reservoirs". Ph.D. thesis, Stanford University, 2012.
- Tahmeen, M., Love, J., Rashidi, B. and Hareland, G.: "Complete geomechanical property log from drilling data in unconventional horizontal wells". ARMA 17-591, The 51st US Rock Mechanics/Geomechanics Symposium, 25-28 June, San Francisco, California, USA, 2017.
- Walls, J. D., Diaz, E., Derzhi, N., Grader, A., Dvorkin, J., Arrendono, S., Carpio, G. and Sinclair, S. W.: "Eagle Ford shale characterization by Digital Rock Physics". 2011 CSPG CSEG CWLS Convention, Houston, TX, USA, 2011.
- Wu, Z. A. and Hareland, G.: "Real-time downhole weight on bit (DWOB) automation in directional drilling". ASME 2015 34th International Conference on Ocean, Offshore and Arctic Engineering, OMAE2015, May 31-June 5, St. John's, Newfoundland, Canada, 2015.
- Zehnder, A. T.: "Fracture Mechanics, Lecture Notes in Applied and Computational Mechanics". Springer Science and Business Media, 2012.

Figures

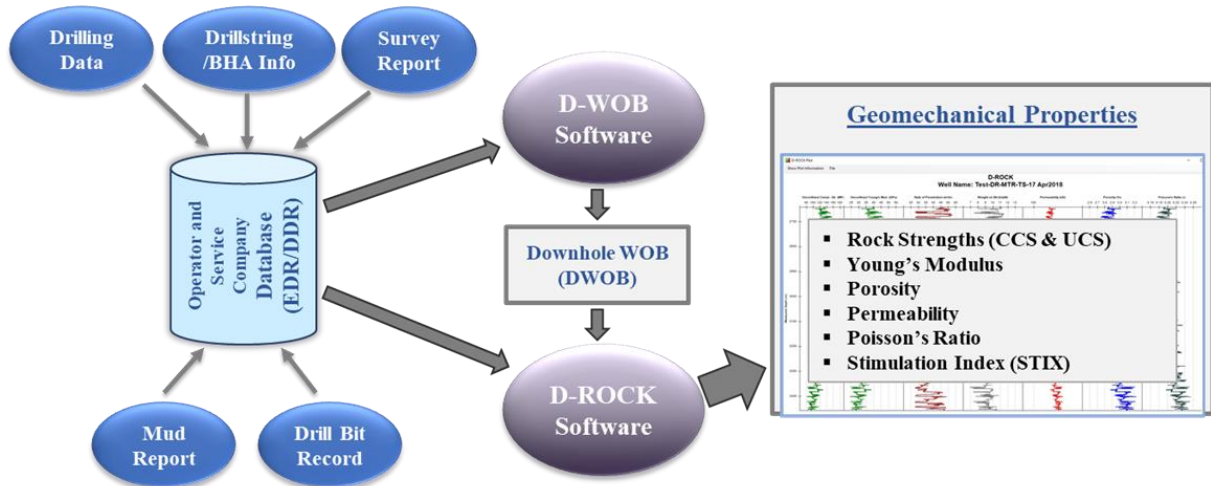


Figure 1. Overview of D-Series technology

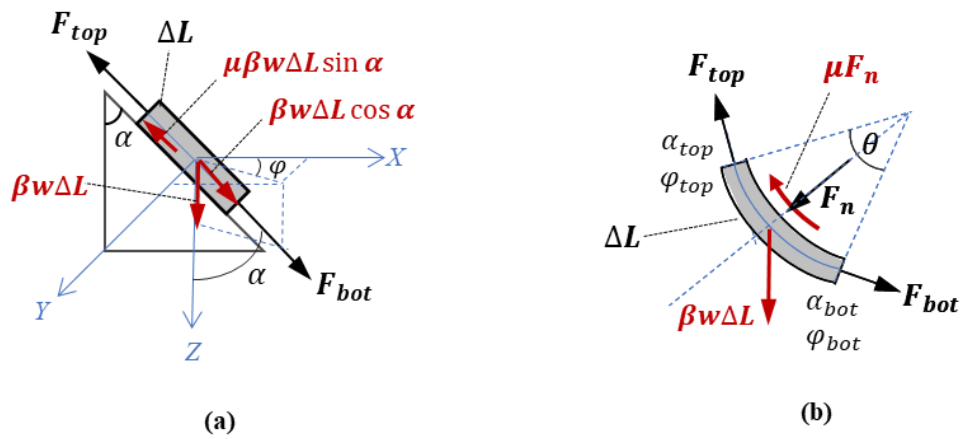


Figure 2. Force balance on drillstring elements

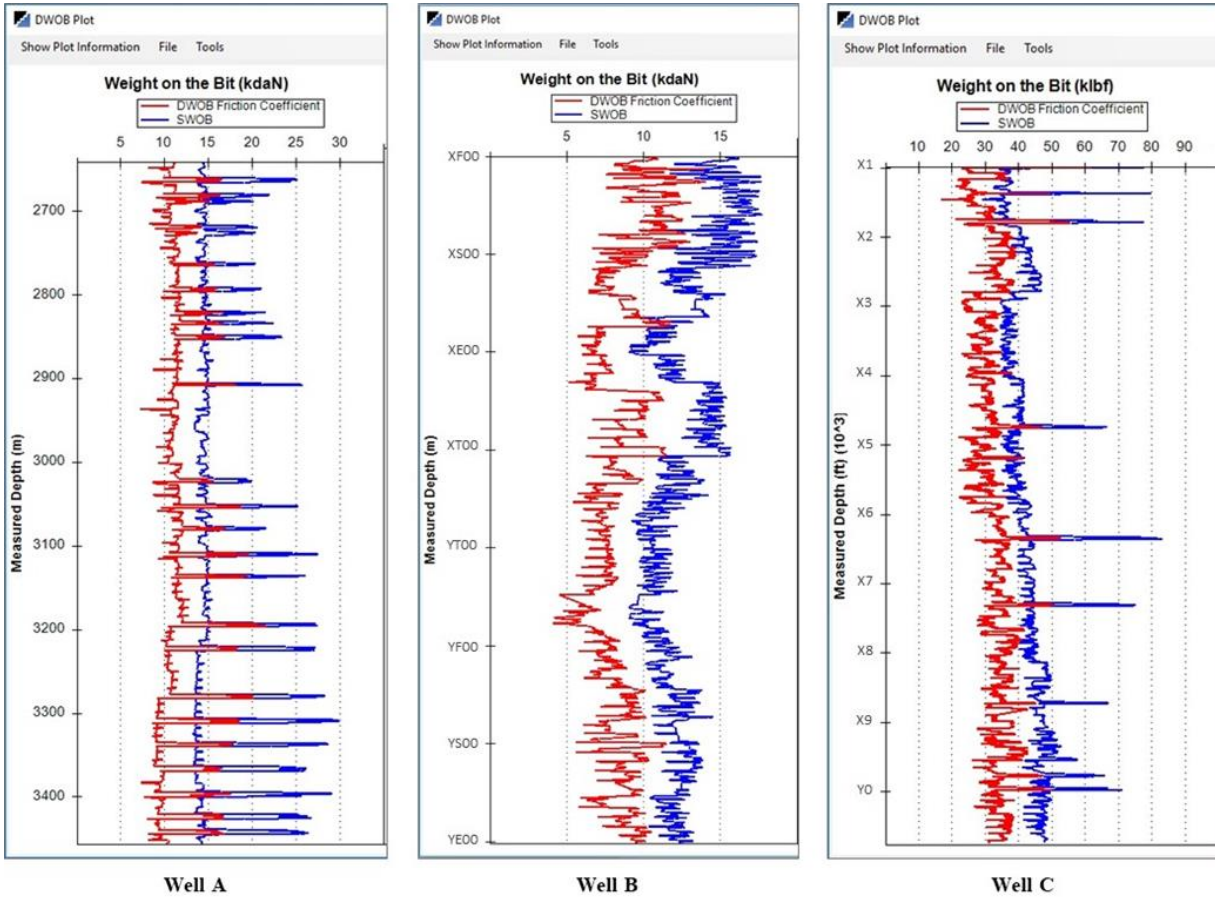


Figure 3. Downhole weight on bit (DWOB) profiles from drilling data

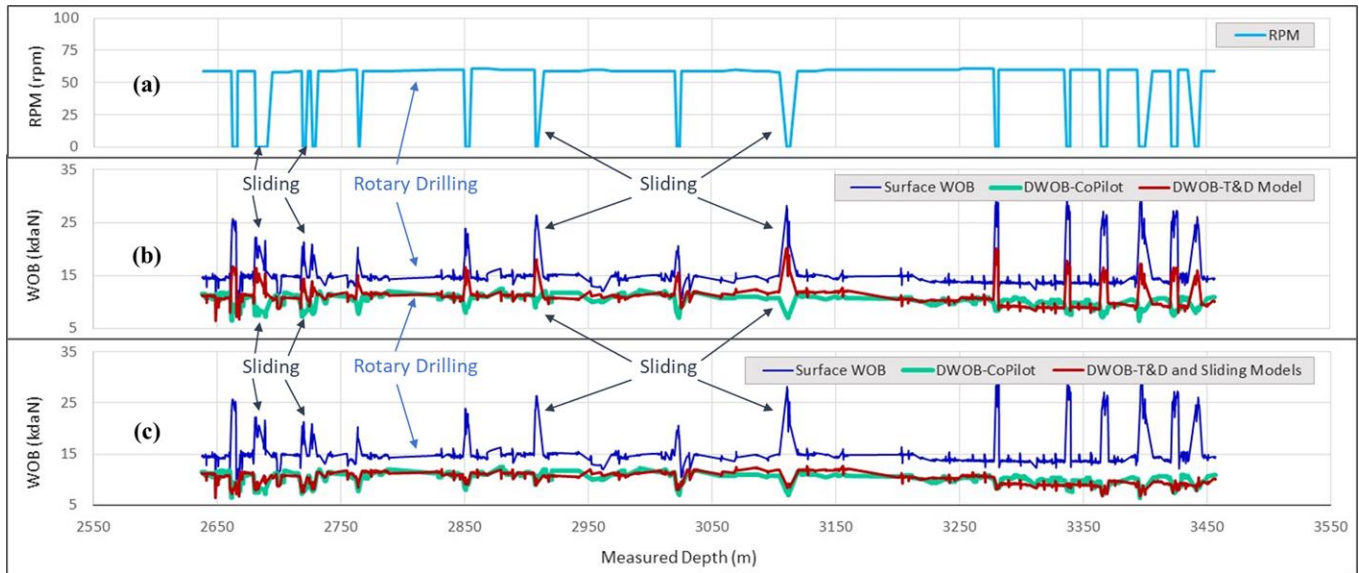


Figure 4. Comparison of the calculated DWOB with the field measurement using the CoPilot downhole tool

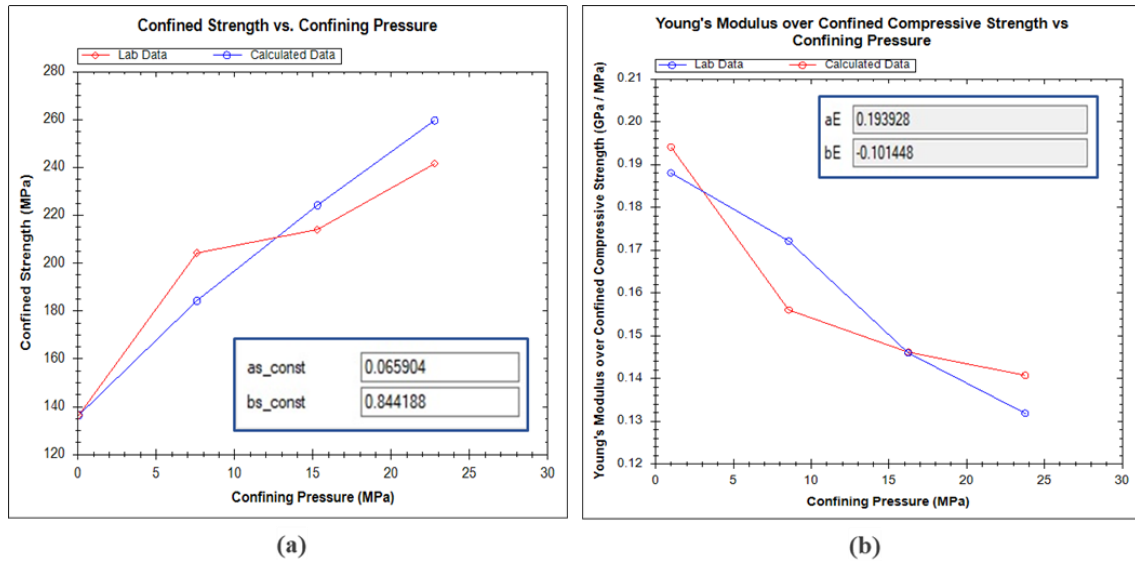


Figure 5. Formation constants obtained from regression analysis utilizing D-ROCK functional tools: (a) and (b) Utilizing D-ROCK functional tools

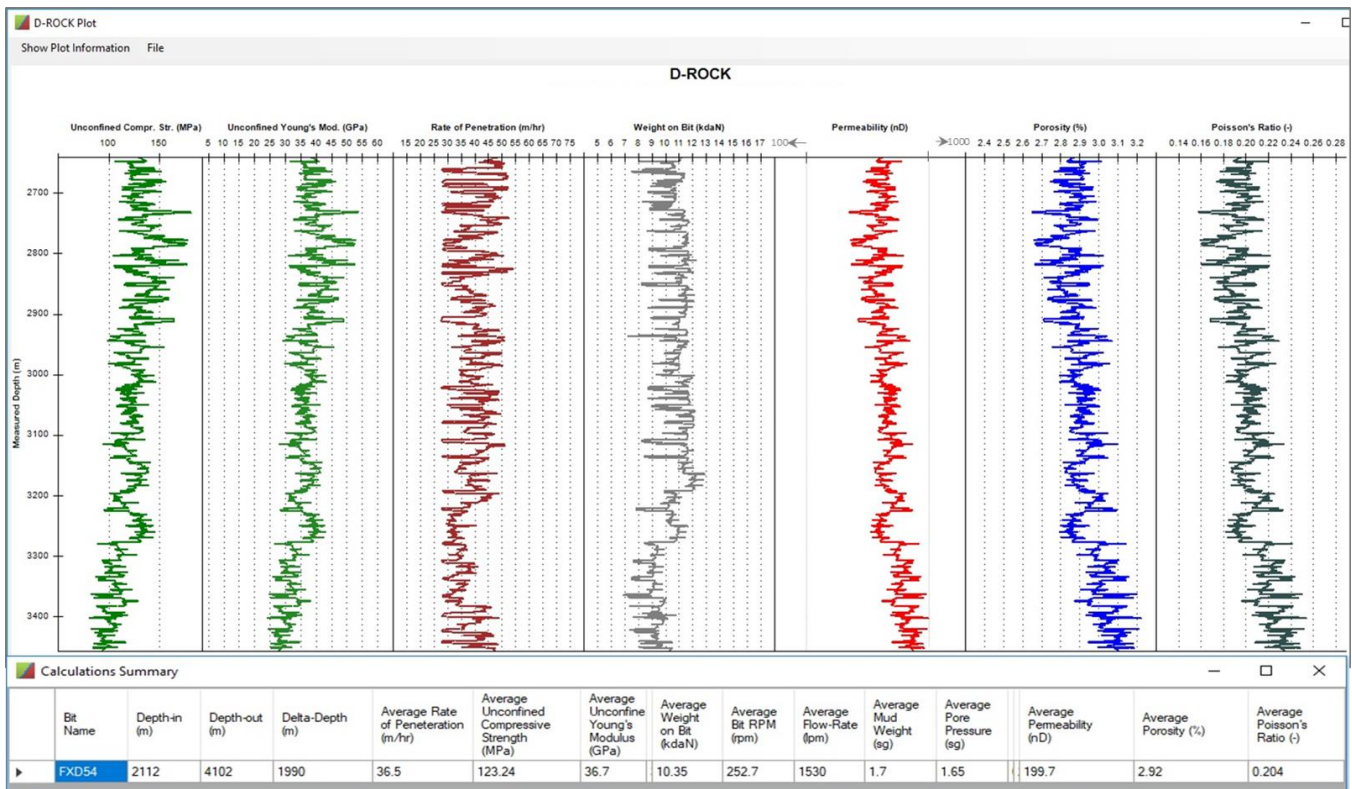


Figure 6: Rock mechanical and reservoir property log utilizing D-ROCK module

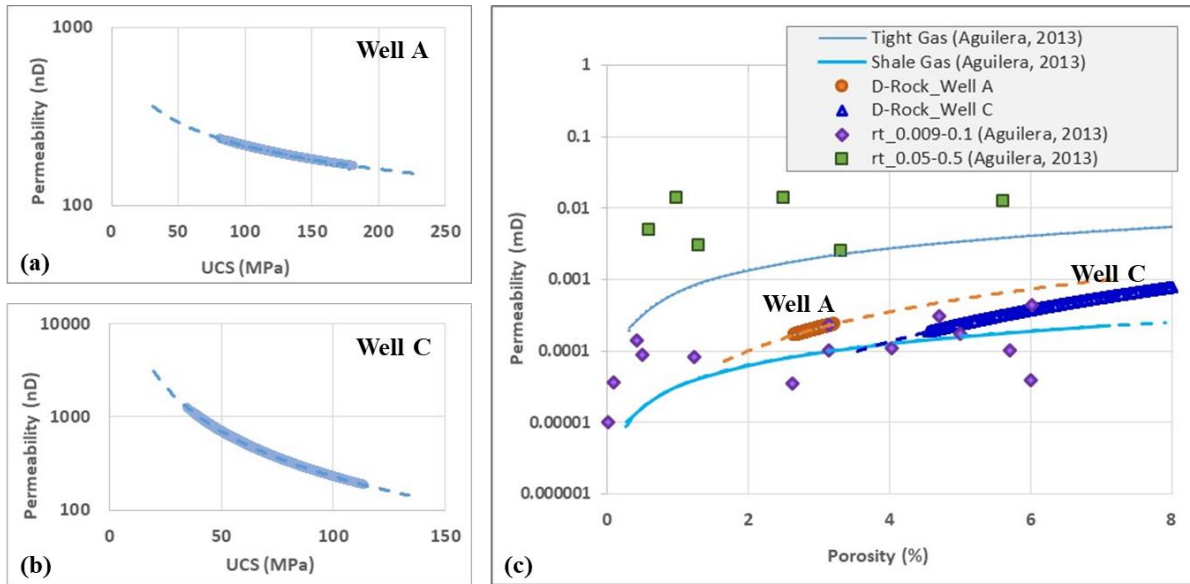


Figure 7: Permeability-UCS and Porosity-Permeability cross-plots: (a) Permeability-UCS for Well A; (b) Permeability-UCS for Well C; (c) verification with the average Shale reservoir trend for flow units (Aguilera, 2013)

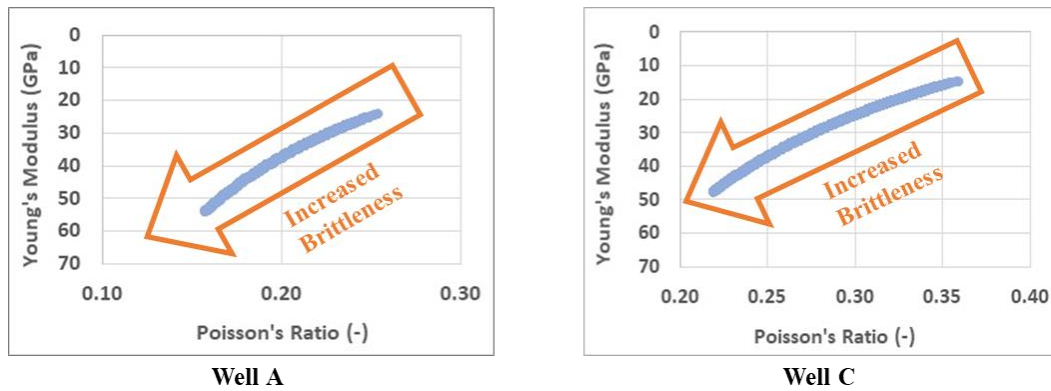


Figure 8. Concept of rock brittleness from the Young's modulus and Poisson's ratio cross-plots

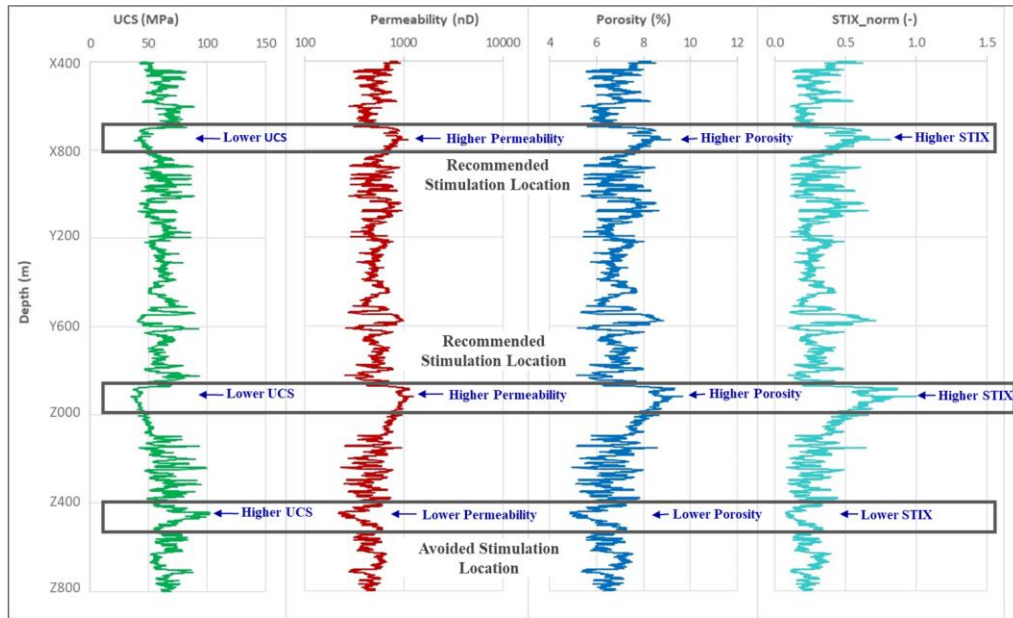


Figure 9. Sample selective stimulation location from the geomechanical property logs (Well C)

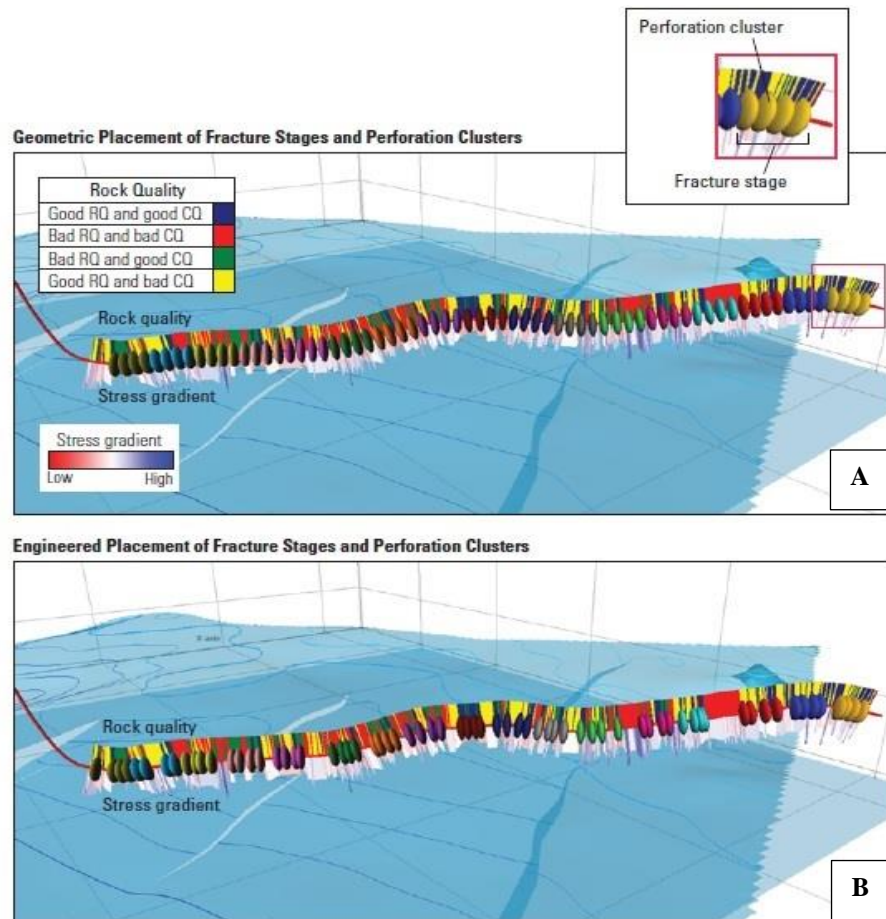


Figure 10. Geometric and engineered designs for a horizontal well in the Eagle Ford formation (Ajayi et al., 2013)

Tables

Table 1. Sample formation constants calculated for the Montney shale formation in NEBC

| Formation Type | Constant ID | Formation Constant |
|---|-------------|--------------------|
| Montney Shale in the North East British Columbia (NEBC), Canada | a_S | 0.065904 |
| | b_S | 0.844188 |
| | a_E | 0.193928 |
| | b_E | -0.101448 |
| | k_{por1} | 9.3373 |
| | k_{por2} | 0.242 |
| | k_{prm3} | 28.573 |
| | k_{prm4} | 1.8132 |

Table 2. Summary of calculated geomechanical properties of unconventional reservoirs

| Shale Formation | Study Well | UCS (MPa) | Young's Modulus (GPa) | Permeability (nD) | Porosity (%) | Poisson's Ratio (-) |
|-----------------|------------|-----------------------------|--------------------------|-----------------------------|--------------------------|-----------------------------|
| NEBC Montney | Well A | 87.9 – 158.8 Avg. 123.24 | 26.4 – 52.8 Avg. 36.7 | 167.8 – 230.9 Avg. 199.7 | 2.67 – 3.22 Avg. 2.92 | 0.158 – 0.254 Avg. 0.204 |
| | Well B | 74.6 -184.4 Avg. 108.56 | 18.5 – 40.1 Avg. 21.1 | 149.2 – 267.9 Avg. 213.7 | 2.54 – 3.42 Avg. 3.03 | 0.159 – 0.310 Avg. 0.234 |
| Eagle Ford | Well C | 53.2 – 129.8 | 16.1 – 41.8 | 273.6 – 1247.4 | 4.26 – 9.29 Avg. 6.59 | 0.221 – 0.356 |

Table 3. Example of nonengineered/geometric and engineered completion summary (Ajayi et al., 2013)

| Well | Completion Summary | | | | 30-Day Cumulative Production | | | |
|----------------------------|--------------------------------|---------------------------------|-------------------------------------|---|------------------------------|--------------------------------------|--|---|
| | Average Treating Pressure, psi | Average Treatment Rate, bbl/min | Placed Proppant per Lateral, lbm/ft | Percentage of Proppant Placed Versus Design | Gross, Mcf | Normalized by Lateral Length, Mcf/ft | Normalized by Number of Stages, Mcf/ft | Normalized by Number of Perforation Clusters, Mcf/cluster |
| Well 1 | 7,749 | 78.1 | 1,783 | 107.0% | 63,194 | 18.7 | 4,514 | 903 |
| Well 2 | 7,557 | 76.3 | 672 | 55.0% | 42,396 | 18.3 | 6,057 | 1,211 |
| Well 3 | 7,716 | 66.3 | 855 | 65.0% | 65,039 | 30.4 | 9,291 | 1,858 |
| Average | 7,674 | 73.6 | 1,103 | 75.7% | 56,876 | 21.8 | 6,094 | 1,219 |
| Well 4 | 7,308 | 79.2 | 1,002 | 92.8% | 212,631 | 47.3 | 17,719 | 3,544 |
| Well 5 | 7,105 | 81.9 | 1,251 | 101.7% | 162,652 | 41.2 | 13,554 | 3,012 |
| Well 6 | 7,298 | 82.3 | 1,245 | 100.5% | 180,436 | 46.0 | 15,036 | 3,341 |
| Average | 7,237 | 81.1 | 1,166 | 98.3% | 185,240 | 44.9 | 15,437 | 3,308 |
| Average difference | -437 | 7.6 | 63 | 22.7% | 128,363 | 23.1 | 9,343 | 2,089 |
| Percent average difference | -5.7% | 10.3% | 5.7% | 30.0% | 226% | 106% | 153% | 171% |